THE UNIVERSITY of EDINBURGH

Edinburgh Research Explorer

Influence of chemical denudation on hillslope morphology

OPEN ACCESS

Influence of chemical denudation on hillslope morphology

Simon Marius Mudd

Department of Civil and Environmental Engineering, Vanderbilt University, Nashville, Tennessee, USA

David Jon Furbish

Departments of Earth and Environmental Sciences and Civil and Environmental Engineering, Vanderbilt University, Nashville, Tennessee, USA

[1] Models of hillslope evolution involving diffusion-like sediment transport are conventionally presented as an equation in which the changes in land-surface elevation or soil thickness are balanced by the divergence of soil transport and tectonic uplift, soil production, or both. These models typically do not include the loss or gain of mass in hillslope soils due to processes of chemical weathering and deposition. We formulate a more general depth-integrated equation for the conservation of soil mass on a hillslope that includes a term representing chemical deposition or denudation. This general depth-integrated equation is then simplified to determine the one-dimensional form of a steady state hillslope which experiences both mechanical and chemical denudation. The differences in morphology between hillslopes only experiencing diffusion-like mechanical sediment transport and hillslopes experiencing both diffusion-like mechanical sediment transport and chemical denudation are explored. Under the conditions of a downslope increase in local soil lowering rate due to chemical weathering the hillslope profile will depart from the parabolic shape predicted by models that incorporate only linear diffusion-like mechanical sediment transport. In addition, hillslopes that experience both chemical and mechanical denudation may have a convex-concave profile at steady state. A necessary condition for such steady state profiles is that the chemical denudation rate must exceed the mechanical denudation rate. We further suggest that combinations of other physical parameter values (such as total denudation rate, average soil depth, sediment diffusivity, and the increase in soil depth away from the divide) that lead to steady state convex-concave hillslope profiles may exist in a wide variety of natural settings. *INDEX TERMS:* 1824 Hydrology: Geomorphology (1625); 1815 Hydrology: Erosion and sedimentation; 1886 Hydrology: Weathering (1625); *KEYWORDS:* hillslope geomorphology, steady state landscapes, weathering

1. Introduction

[2] Landscapes that contain topographic relief are often mantled with soil. In a seminal paper, *Gilbert* [1909] remarked that downslope motion of sediment on a hillslope is impelled by gravity, which depends on slope for its effectiveness. Furthermore, *Gilbert* [1909] noted that in order to accommodate increasing downslope sediment flux, the transport rate of sediment should increase away from the hillslope divide, and therefore the local slope should steepen away from the divide. The result of this steepening slope is the presence of a convex hillslope (Figure 1). *Culling* [1960] formalized this observation mathematically by combining a sediment flux law and a statement of mass conservation. The flux law used by *Culling* [1960], in which the sediment flux is a linear function of the surface elevation gradient, was analogous to the heat flux law

introduced by *Fourier* [1822]; such gradient-driven processes are referred to as diffusive. Since the publication of *Culling*'s [1960] work, other researchers have proposed nonlinear flux laws [e.g., *Anderson*, 2002; *Andrews and Bucknam*, 1987; *Carson and Kirkby*, 1972; *Furbish and Fagherazzi*, 2001; *Gabet*, 2000, 2003; *Gabet et al.*, 2003; *Kirkby*, 1967; *Roering et al.*, 1999]. Because the analogy to heat or chemical diffusion is not perfect, the family of flux laws describing hillslope sediment transport is now more appropriately referred to as dispersive or "diffusion-like."

[3] The equations of diffusion-like hillslope sediment transport have been used to investigate the dynamics and implications of hillslope morphology and evolution. Some researchers have used these equations to explore the characteristic forms of steady state or equilibrium hillslopes and the adjustment times from transient profiles to steady state profiles [e.g., *Ahnert*, 1976, 1987; *Armstrong*, 1976, 1980, 1987; *Arrowsmith et al.*, 1996; *Fernandes and Dietrich*, 1997; *Furbish and Fagherazzi*, 2001; *Hirano*, 1976; *Roering et al.*, 1999]. In these studies, steady state refers to a situation
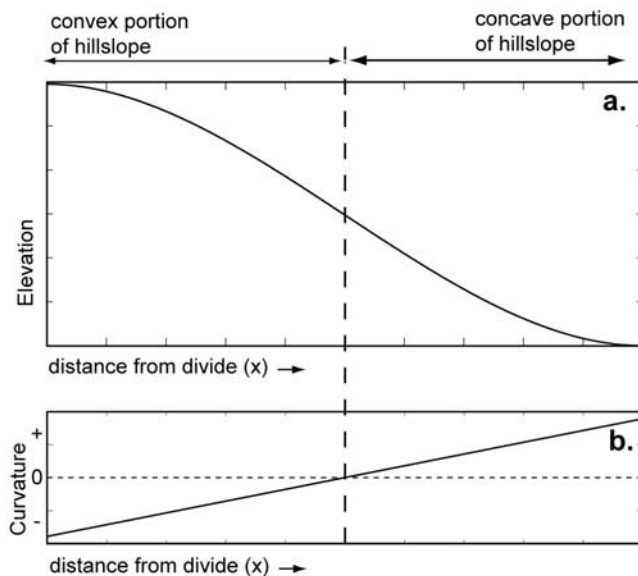
Figure 1. (a) An idealized convex-concave hillslope. The convex portion has negative curvature by convention, and the concave portion has positive curvature. (b) Slope curvature.

in which the elevation of the soil surface does not change through time. This surface elevation can be the elevation in a moving reference frame in the case of steady base-level fall or in a fixed reference frame in the case of steady uplift. Others have used a steady state assumption to investigate the mechanics and nature of soil production [e.g., *Heimsath et al.*, 1999]. These studies assume that soil depth does not change through time. As pointed out by *Braun et al.* [2001], this definition of steady state does not necessarily imply topographic steady state. Others [e.g., *Anderson and Dietrich*, 2001] have defined steady state as a condition in which a broad range of physical characteristics of the soil, such as soil density, soil chemistry, and soil depth, in addition to surface elevation, do not vary with time.

[4] Another group of researchers has used the most basic forms of the equations of hillslope sediment transport (typically linear flux laws with threshold slopes) in models of landscape evolution [e.g., *Anderson*, 1994; *Braun and Sambridge*, 1997; *Howard*, 1994, 1997; *Kooi and Beaumont*, 1994; *Tucker and Slingerland*, 1996; *Willgoose et al.*, 1991]. *Tucker and Bras* [1998] found that a landscape's morphology is highly sensitive to the suite of mechanisms of sediment transport operating within it.

[5] As anticipated by *Gilbert* [1909], analytic and numerical solutions of the equation of mass conservation on hillslopes with diffusion-like sediment transport have shown that with steady base-level fall, hillslope profiles will have negative curvature (indicating a convex hillslope (see Figure 1)). Predicted hillslope curvature can approach zero (a locally planar hillslope) if a nonlinear diffusion-like sediment flux law is used [*Roering et al.*, 1999]. In rapidly uplifting landscapes such as the Oregon Coast Range or Central Range of Taiwan the hillslopes are commonly convex near the divide and planar down-slope [*Roering et al.*, 1999]. Concavity on hillslopes with steady base-level fall may be caused by processes such as sheetwash [e.g., *Ahnert*, 1976; *Kirkby*, 1971], but in

landscapes with gentler slopes or high infiltration capacities, overland flow is uncommon and not an effective process of geomorphic change.

[6] Hillslope concavity is often seen in landscapes where overland flow is uncommon. In such landscapes the concavity has been identified as a location of sediment deposition and storage [e.g., *Armstrong*, 1987]. The deposition of sediment reflects a transient state. In a two-dimensional (2-D) numerical model, *Rinaldo et al.* [1995] investigated unchanneled valleys, where there is landscape concavity but no fluvial channel to maintain the concavity. *Rinaldo et al.* [1995] described these unchanneled valleys as indicators of climatic or tectonic change. If the climate becomes ''drier'' (in the work of *Rinaldo et al.* [1995] a drier climate simply indicated that a greater drainage area was required for fluvial erosion), uplift is reduced, or the runoff threshold (the amount of rain that must fall before overland flow is generated) is increased due to changes in the biota present on the landscape, the fluvial system retreats downstream, and diffusion-like hillslope processes begin depositing sediment and filling unchanneled valleys. Unless the sediment filling these valleys is evacuated by a fluvial network that has expanded due to climate change, the valleys will be smoothed from the landscape (Figure 2).

[7] The timescale of the gradual smoothing away of landscape concavities (such as an unchanneled valley in the 2-D case (Figure 2)) on hillslopes experiencing only diffusion-like sediment transport is dictated by the relaxation time of the hillslope. The relaxation time of a hillslope has been defined as the time it takes for a hillslope to approach an equilibrium state after a change in climate (represented by a change in the sediment diffusivity) or a change in base-level lowering rate [*Fernandes and Dietrich*, 1997; *Roering et al.*, 2001]. Relaxation times for hillslopes with typical diffusivities have been found to be on the order of 10^4-10^6 years [*Fernandes and Dietrich*, 1997; *Roering et al.*, 2001; *Anderson*, 2002]. Many ancient landscapes, such as the Piedmont of the eastern United States, have widespread landscape concavities. Why have the unchanneled valleys and landscape concavities in these ancient landscapes not been filled by hillslope processes? Are landscapes containing unchanneled valleys diffusing away to a Davisian [*Davis*, 1889] peneplain? Despite a drastically reduced rate of base-level fall, can landscape concavities persist solely due to the effects of climatic fluctuations?

[8] One explanation for the presence of long-lived landscape concavity is that it is periodically rejuvenated by episodes of wet weather or other climatic or biotic changes that cause the expansion of the channel network and erosion of sediment-filled valleys [*Rinaldo et al.*, 1995]. We suggest, however, that in addition to the theory of *Rinaldo et al.* [1995], there exists another plausible explanation of concavity in landscapes older than the hillslope relaxation time. We show that the convex-concave hillslope can exist in an equilibrium state due to a process that has been largely ignored in previous hillslope evolution studies. This process is mass loss in the soil due to chemical weathering. We derive an depth-integrated equation of mass conservation in hillslope soils that includes the mass lost or gained through chemical processes. This equation is simplified to 1-D and

is used to investigate how chemical processes may affect the curvature, slope, and form of hillslopes. We explore the combinations of physical parameter values including total denudation rate, sediment diffusivity, the increase in soil depth away from the divide, and the ratio of the mechanical to chemical denudation rate that lead to a convex-concave profile at steady state. We further suggest that these combinations of parameters associated with a steady state convex-concave hillslope profile may exist in a wide variety of natural settings.

2. A Depth-Integrated Equation of Hillslope Mass Conservation Incorporating Chemical Denudation and Deposition

2.1. Previous Work

[9] Before the implications of chemical weathering on hillslope morphology can be investigated, the equation of hillslope sediment transport incorporating this process must be derived. Few researchers have addressed the processes of chemical weathering, denudation, or deposition in their analysis. *Furbish and Fagherazzi* [2001] proposed a heuristic alteration of the soil production function as described by *Heimsath et al.* [1997] to account for weathering. *Ahnert* [1987] included dissolved load denudation derived from slope wash but calculated this chemical denudation as a function of the overland flow and not as weathering and transport occurring within the soil profile. *Small et al.* [1999] used a dissolution term in a steady state form of the equation of mass conservation on a hillslope to show that dissolution can affect ages determined by cosmogenic radionuclides but did not explore the implications of denudation on hillslope morphology. Likewise, *Kirkby* [1977, 1985] modeled soil chemistry evolution within a creeping soil but only

reported modeled vertical soil profiles and did not comment on the expression of these processes on the morphology of the hillslopes in question.

2.2. General Statement of Mass Conservation

[10] Researchers typically report the hillslope diffusion-like equations as a specific case of a more general statement

Figure 2. Idealized simulation of a soil-mantled landscape using a traditional form of the sediment continuity equation, $\rho_s \left(\partial \zeta / \partial t \right) - K \nabla^2 \zeta - \rho_r U_z = 0$. Terms are defined in the text. Values for the parameters are $\rho_r = 2000$ kg^{-3}, $\rho_s = 1000$ kg^{-3}, $R_T = 1 \times 10^{-5}$ m yr^{-1}, and $K = 10$ kg yr^{-1} ($D = 1 \times 10^{-2}$ m^2 yr^{-1}). The domain represents a straight main stem channel that is eroding at the rate of uplift ($\partial \zeta / \partial t = 0$) and transporting all sediment delivered to it. Two additional tributary channels with exponential profiles are initially imposed on the hillslope; these channels are also eroding at the rate of uplift and transporting all sediment delivered to them. This landscape is then brought to steady state ($\partial \zeta / \partial t = 0$ everywhere), as shown in Figure 2a. The tributary channels then recede (no fluvial erosion or transport), and only the main stem channel erodes at the rate of uplift. The valleys fill significantly by 250 ka (Figure 2b), and the unchanneled valleys almost completely disappear from the landscape by 750 ka after imposition of the new conditions (Figure 2c). Figure 2d shows profiles parallel to the main stem at a distance of 250 m from the divide. At steady state the curvature of the side slopes are negative, resulting in a convex hillslope form. Only when the tributary channels are removed does there appear a concave section of the side slope, representing deposition and filling of the unchanneled valleys (Figure 2d).
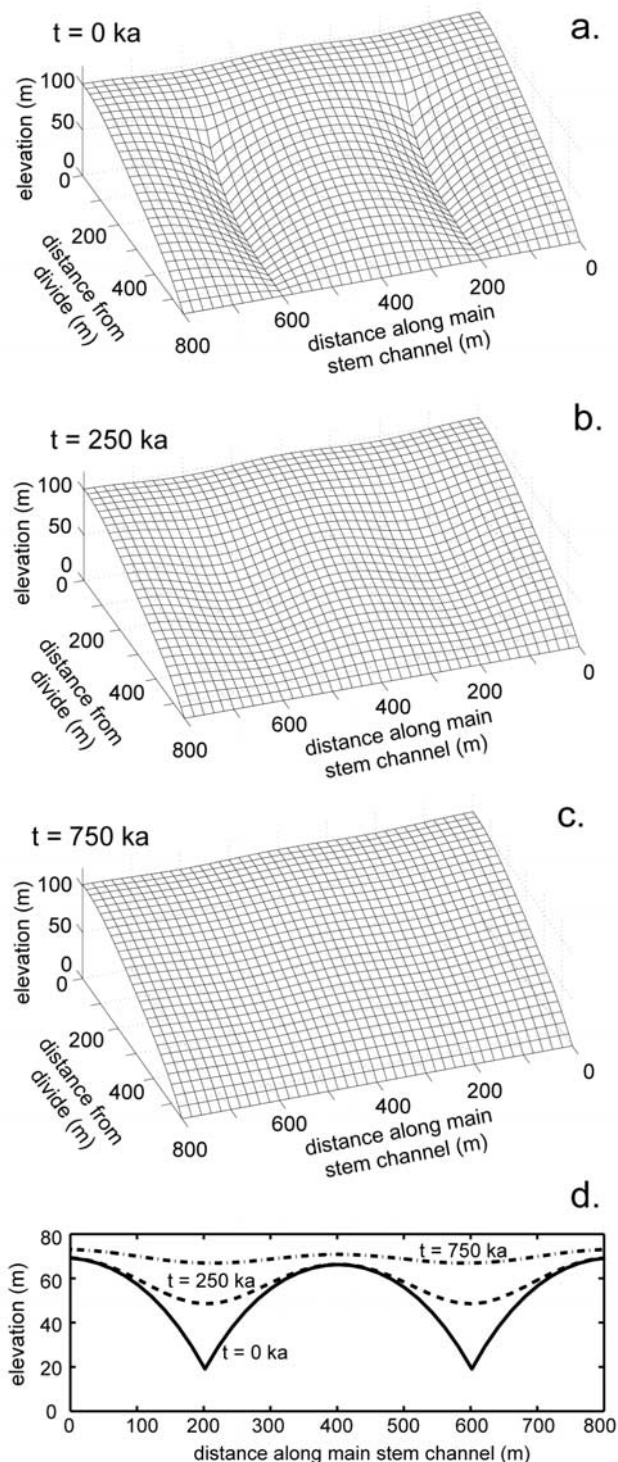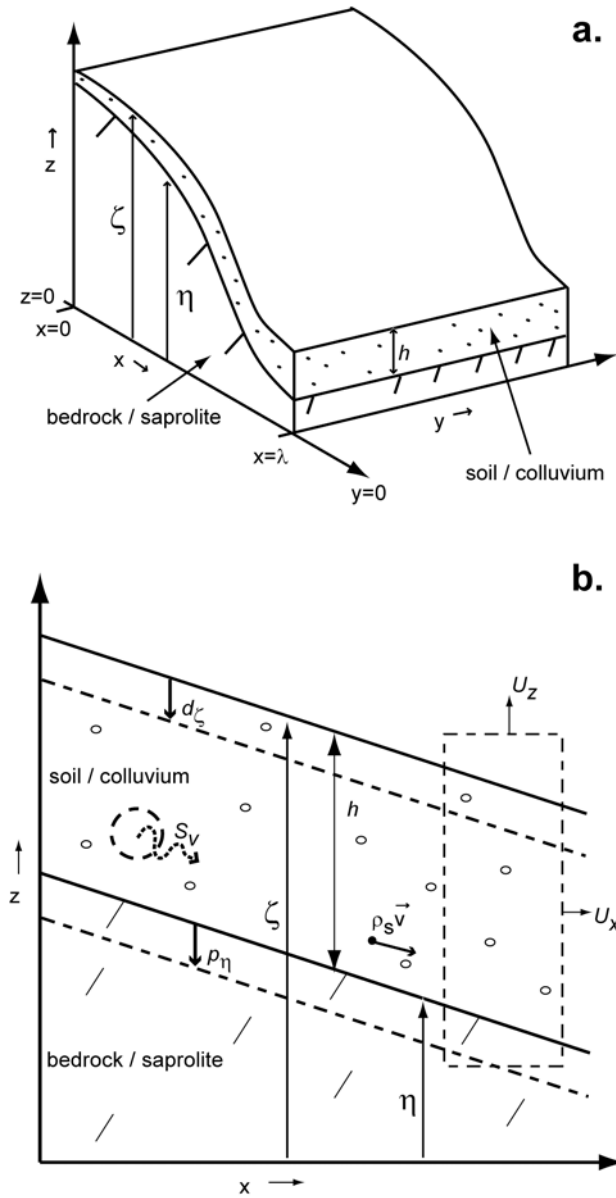
Figure 3. Diagrams of coordinate system adopted for soil-mantled hillslopes. If the surfaces $z = \eta$ and $z = \zeta$ change as shown in Figure 3b, then the production rate (p_η) is positive, and that deposition rate (d_ζ) is negative.

of local mass conservation. This specific case is generally assumed a priori. Here we derive the equation for conservation of mass on a hillslope directly from a local statement of mass conservation. We begin with the familiar continuum element with a surface A (L^2), a volume V (L^3), and a vector normal to the surface **n** (L). A generalized form of the local conservation of mass in this element is

$$\int_V \frac{\partial}{\partial t} \rho_s dV + \int_A (\rho_s \mathbf{v}) \cdot \mathbf{n} dA - \int_V S_v dV = 0, \qquad (1)$$

where ρ_s (ML^{-3}) is the dry bulk density of the soil and **v** (LT^{-1}) is the velocity vector of the material at the surface of the element. The velocity will be an ensemble average velocity of the discrete particles crossing the surface of the

continuum element (Figure 3). The first term is the change in mass per unit volume per unit time of the material in the continuum element, and the second term is the flux of mass per unit volume across the surface of the element. S_v $(ML^{-3}T^{-1})$ is a mass source or sink per unit volume per time and will be referred to as the chemical denudation and/ or deposition rate. Equation (1) is used here to describe the local conservation of mass in the solid phase of a hillslope soil. The local soil mass can change due to dissolution into or precipitation from the aqueous phase, which is described by the source or sink term. This term allows the equation of soil mass conservation to be coupled to advection-dispersion-reaction (ADR) equations, which describe solute concentration for chemical species in the aqueous phase. This coupling is beyond the scope of this contribution but will be important in future research. Coupling equation (1) to the ADR equations is not necessary for significant details of hillslope form and process to be interpreted through equation (1).

[11] The velocity vector in equation (1) can be decomposed into tectonic velocity, **U** (LT^{-1}) and local soil velocity $\mathbf{v}_s$ (LT^{-1}):

$$\int_V \frac{\partial}{\partial t} \rho_s dV + \int_A [\rho_s (\mathbf{v}_s + \mathbf{U})] \cdot \mathbf{n} dA - \int_V S_v dV = 0. \qquad (2)$$

Invoking Gauss's law, the flux term (the second term) is converted to a volume integral, after which the resulting integral can be differentiated to

$$\frac{\partial \rho_s}{\partial t} + \nabla \cdot (\rho_s \mathbf{v}_s) + \nabla \cdot (\rho_s \mathbf{U}) - S_v = 0. \qquad (3)$$

Equation (3) may be written in component form:

$$\frac{\partial \rho_s}{\partial t} + \frac{\partial (\rho_s v_{sx})}{\partial x} + \frac{\partial (\rho_s v_{sy})}{\partial y} + \frac{\partial (\rho_s v_{sz})}{\partial z} + \frac{\partial (\rho_s U_x)}{\partial x} + \frac{\partial (\rho_s U_y)}{\partial y}$$
$$+ \frac{\partial (\rho_s U_z)}{\partial z} - S_v = 0, \qquad (4)$$

where the subscripts x, y, and z denote the components of the sediment and tectonic velocity vectors in the x, y, and z directions, respectively (Figure 3).

2.3. Depth Integration of the Statement of Mass Conservation

[12] Coordinates for the surface of the soil ($z = \zeta$) and the base of the active soil ($z = \eta$) are adopted (Figure 3). Soil scientists, geomorphologists, and geologists may use different definitions for the words regolith, soil, saprolite, and bedrock. The definition of soil adopted here is that part of the material at the near surface that is being actively disturbed by mechanical means: the active layer. The active layer will extend to the deepest of the rooting depth, burrowing depth, creep depth, shrink-swell depth, or frost-heave depth. This is different from the traditional definitions of soil and bedrock, but here the definitions reflect the emphasis on the physics of transport. The terms "mechanically active layer" and "mechanically inactive layer" may be more appropriate, but in many natural settings the soil and the saprolite (or bedrock) coincide with the active and inactive layers, respectively, so these terms are retained.

[13] Equation (4) may then be depth integrated between ζ and η:

$$\int_{\eta}^{\zeta} \frac{\partial \rho_s}{\partial t} dz + \int_{\eta}^{\zeta} \frac{\partial (\rho_s v_{sx})}{\partial x} dz + \int_{\eta}^{\zeta} \frac{\partial (\rho_s v_{sy})}{\partial y} dz + \int_{\eta}^{\zeta} \frac{\partial (\rho_s v_{sz})}{\partial z} dz$$
$$+ \int_{\eta}^{\zeta} \frac{\partial (\rho_s U_x)}{\partial x} dz + \int_{\eta}^{\zeta} \frac{\partial (\rho_s U_y)}{\partial y} dz + \int_{\eta}^{\zeta} \frac{\partial (\rho_s U_z)}{\partial z} dz$$
$$- \int_{\eta}^{\zeta} S_v dz = 0. \tag{5}$$

The soil depth h is the distance between the surface and base of the soil:

$$h = \zeta - \eta. \tag{6}$$

The integrals in equation (5) are evaluated using the mean value theorem and Leibniz's rule (Appendix A).

2.4. Kinematic Conditions at the Soil Surface and the Soil-Bedrock Boundary

[14] The use of Leibniz's rule in equation (5) results in a number of terms that are evaluated at the coordinates $z = \zeta$ and $z = \eta$. These terms must be addressed by assigning kinematic boundary conditions. These are the conditions that describe the motion of the soil surface and the soil-bedrock boundary. The kinematic boundary condition at $z = \zeta$ is

$$\frac{\partial \zeta}{\partial t} = (v_{sz} + U_z)\Big|_{\zeta} - (v_{sx} + U_x)\Big|_{\zeta} \frac{\partial \zeta}{\partial x} - (v_{sy} + U_y)\Big|_{\zeta} \frac{\partial \zeta}{\partial y} + d_\zeta. \tag{7}$$

The first term to the right of the equality is the vertical velocity at the soil surface. The second and third terms result from the fact that a particle must remain on the soil surface even if it has horizontal velocity. If a particle that remains on the surface moves to a location with a different surface coordinate, it must have some component of vertical velocity. The last term to the right of the equality, d_ζ (LT^{-1}), is a deposition or erosion term. This term can describe deposition from organic or aeolian sources or erosion from overland flow. It should be noted that this term describes mass being transported in or out of the hillslope sediment system. This term allows coupling of the hillslope sediment transport equation to transport equations for overland flow. Processes in which sediment only briefly leaves the system but over the long term resides on the hillslope, such as rain splash, should be accounted for in the flux terms in the hillslope sediment conservation equation. Additionally, in some cases the leaf layer may not be considered part of the soil profile. Organic carbon in the soil is left by the decay of roots within the soil and leaching of carbon from the leaf litter layer into the underlying soil. In these cases the mass contributed to the soil from organic carbon would be encompassed by the chemical denudation and deposition term.

[15] The kinematic boundary condition at the soil-bedrock interface is

$$\frac{\partial \eta}{\partial t} = U_z\Big|_{\eta} - U_x\Big|_{\eta} \frac{\partial \eta}{\partial x} - U_y\Big|_{\eta} \frac{\partial \eta}{\partial y} - p_\eta. \tag{8}$$

The sediment velocities in the x, y, and z directions at this boundary are zero, but tectonic velocities are nonzero. The term p_η (LT^{-1}) will be positive if the active layer lowers in the absence of tectonic velocities. One cause of lowering of the active layer is soil production, which is the conversion of bedrock or saprolite to soil through chemical, biological, or mechanical processes [e.g., *Heimsath et al.*, 1997].

2.5. Depth-Integrated Equation for Mass Conservation of Soil on a Hillslope

[16] After depth integration, the equation for mass conservation of soil on a hillslope is

$$\frac{\partial}{\partial t} (h\bar{\rho}_s) + \frac{\partial}{\partial x} (h\overline{\rho_s v_{sx}}) + \frac{\partial}{\partial y} (h\overline{\rho_s v_{sy}}) + \frac{\partial}{\partial x} (h\overline{\rho_s U_x}) + \frac{\partial}{\partial y} (h\overline{\rho_s U_y})$$
$$- h\bar{S}_v - \rho_s|_{\eta}(p_\eta) - \rho_s|_{\zeta}(d_\zeta) = 0. \tag{9}$$

The overbar denotes a depth-integrated quantity. The quantity d_ζ is positive for deposition and negative for erosion, and the quantity $\bar{S}_v$ is negative in the case of dissolution and positive in the case of precipitation. Figure 3 shows the coordinate system and components of equation (9). The dry bulk density at the soil-bedrock boundary, or $\rho_s|_{\eta}$, is renamed ρ_r. The dry bulk density of the soil at the surface, or $\rho_s|_{\zeta}$, is renamed ρ_ζ. The second and third terms in equation (9) contain sediment flux terms:

$$\overline{\rho_s v_{sx}} = q_{sx} \tag{10a}$$

$$\overline{\rho_s v_{sy}} = q_{sy}. \tag{10b}$$

The sediment fluxes q_{sx} and q_{sy} have units $ML^{-2}T^{-1}$. The subscripts x and y denote flux in the x and y directions, respectively. Substituting equations (10a) and (10b) into equation (9) yields

$$\frac{\partial}{\partial t} (h\bar{\rho}_s) + \frac{\partial}{\partial x} (hq_{sx}) + \frac{\partial}{\partial y} (hq_{sy}) + \frac{\partial}{\partial x} (h\overline{\rho_s U_x}) + \frac{\partial}{\partial y} (h\overline{\rho_s U_y})$$
$$- h\bar{S}_v - \rho_r p_\eta - \rho_\zeta d_\zeta = 0. \tag{11}$$

Equation (11) may be written in vector form:

$$\frac{\partial}{\partial t} (h\bar{\rho}_s) + \nabla_2 \cdot (h\mathbf{q_s}) + \nabla_2 \cdot (h\overline{\rho_s \mathbf{U}}) - h\bar{S}_v - \rho_r p_\eta - \rho_\zeta d_\zeta = 0. \tag{12}$$

In equation (12), all vectors and vector operators are in the x and y directions only, for example, $\nabla_2 = \mathbf{i}\partial/\partial x + \mathbf{j}\partial/\partial y$, where $\mathbf{i}$ is the unit vector in the x direction and $\mathbf{j}$ is the unit vector in the y direction.

2.6. Simplifying Assumptions for Conservation of Mass Equation

[17] Equation (12) is a general form of the equation of hillslope sediment continuity. Various forms of this equation may be derived using simplifying assumptions. An almost universal assumption in studies of hillslope geomorphology is that the local horizontal tectonic motions are zero, or $U_x = U_y = 0$. There are some examples of research at the

mountain belt scale in which horizontal tectonic velocities have been incorporated into a surface processes model [e.g., *Ellis et al.*, 1999; *Willett et al.*, 2001] but to the authors' knowledge, none at the hillslope scale. The assumption of zero horizontal tectonic velocities may be inappropriate in some settings, such as small folds or basins, in which the folding or extension is occurring at the scale of the hillslope. A hillslope growing over a low angle blind thrust fault should have significant horizontal tectonic velocities relative to vertical velocities [e.g., *Keller et al.*, 1998]. For many situations, however, an assumption of zero horizontal tectonic velocities, such as landscapes undergoing long wavelength flexure or isostatic rebound, will be appropriate.

[18] It is typically assumed a priori that deposition from organic or aeolian sources is zero. Additionally, slope wash is often not considered because it is a channelizing process rather than a diffusion-like process [e.g., *Ahnert*, 1987] (although it has been shown that overland flow can lead to landscape convexity under the proper conditions [*Dunne*, 1991]). In either of the above cases the deposition term is set to zero. Setting deposition to zero and assuming no horizontal tectonic velocities leads to

$$\frac{\partial}{\partial t}(h\bar{\rho}_s) + \nabla_2 \cdot (h\mathbf{q}_s) - h\bar{S}_v - \rho_r p_\eta = 0. \qquad (13)$$

A version of equation (13) expressed in terms of the rate of change in the land surface elevation is presented in Appendix B.

3. Steady State, Chemically Denuding Hillslope: One-Dimensional (1-D) Analysis

[19] We investigate the effects of chemical processes on hillslope form by using the limited but illustrative case of the one-dimensional hillslope at steady state (to be defined in section 3.1).

3.1. Derivation of Governing Equations

[20] Equation (13) may be cast in its one-dimensional form:

$$\frac{\partial}{\partial t}(h\bar{\rho}_s) + \frac{\partial}{\partial x}(hq_{sx}) - h\bar{S}_v - \rho_r p_\eta = 0. \qquad (14)$$

This equation can be simplified by making steady state assumptions. The first of these assumptions is that the depth-integrated dry bulk density of the soil is spatially and temporally homogenous. This implies (if the density of the mineral grains that make up the soil is not changing) that the porosity of the soil remains constant in time and space. Soils may be maintained at a constant porosity because mechanical disturbances such as bioturbation will collapse excess porosity created by mass losses due to chemical weathering [*Brimhall et al.*, 1992]. The second assumption is that the soil depth does not change in time ($\partial h/\partial t$). This eliminates the first term in equation (14). The next assumption involves defining elevations relative to a local base level:

$$\frac{\partial \eta_{bl}}{\partial t} = \frac{\partial \eta}{\partial t} - \frac{\partial \eta_\lambda}{\partial t} \qquad (15a)$$

$$\frac{\partial \zeta_{bl}}{\partial t} = \frac{\partial \zeta}{\partial t} - \frac{\partial \eta_\lambda}{\partial t}, \qquad (15b)$$

where the subscript *bl* indicates an elevation relative to base level and η_λ is the elevation of the base level. The second

assumption in our definition of steady state is that the elevations relative to base level are not changing in time, or $\partial \eta_{bl}/\partial t = \partial \zeta_{bl}/\partial t = 0$. This is the case of steady topographic form implied by *Gilbert* [1909]. The result of this assumption is that the elevation of the soil-bedrock boundary and the elevation of the soil surface anywhere on the hillslope are changing at the same rate as the elevation of local base level. It is assumed that the tectonic uplift rate is spatially homogenous at the hillslope scale. If U_z and $\partial \eta/\partial t$ are spatially homogenous, then p_η is also spatially homogenous.

[21] To maintain the steady state defined above, all the soil entering the active layer on the hillslope must be removed by either mechanical or chemical processes. In other words, p_η will equal the total denudation rate:

$$p_\eta = R_c + R_m = R_T, \qquad (16)$$

where R_c is the chemical denudation rate (LT^{-1}), R_m is the mechanical denudation rate (LT^{-1}), and R_T is the total denudation rate (LT^{-1}). Incorporating the assumptions stated above, equation (14) becomes

$$\frac{\partial}{\partial x}(hq_{sx}) = h\bar{S}_v + \rho_r R_T. \qquad (17)$$

[22] At this point a constitutive equation for sediment flux must be chosen. Two field studies have found evidence for a linear sediment transport law on gentle slopes [*Mckean et al.*, 1993; *Small et al.*, 1999]. A linear formulation also allows analytic solutions for equation (17). Although there is evidence that nonlinear sediment transport laws may be operating on many natural hillslopes [*Roering et al.*, 1999], a linear sediment transport law is a reasonable approximation on gently sloping hillslopes and is used in this study. The linear sediment transport equation is

$$h\mathbf{q}_s = -\bar{\rho}_s D \nabla_2 \zeta, \qquad (18)$$

where D ($L^2 T^{-1}$) is a sediment diffusivity. (Another coefficient occasionally reported in the literature, K, is in units of $ML^{-1}T^{-1}$. This coefficient is related to D by $K = \bar{\rho}_s D$.) It is assumed that D is spatially homogenous. Equation (18) is inserted into equation (17), and the resulting equation is divided by $\bar{\rho}_s$ to give

$$D\frac{\partial^2 \zeta}{\partial x^2} + \frac{h\bar{S}_v}{\bar{\rho}_s} + \frac{\rho_r}{\bar{\rho}_s}R_T = 0. \qquad (19)$$

Each of the three terms in equation (19) are rates in units LT^{-1}. These are the local rates of change of the surface elevation due to diffusion-like sediment transport, chemical denudation or deposition, and p_η. Again, p_η is replaced by the total denudation rate because we have assumed steady topographic form. The total denudation rate represents a rate of lowering for material with density ρ_r, whereas terms in equation (19) represent soil lowering rates. This is why the total denudation rate in the third term of equation (19) is multiplied by a density ratio. The modeled hillslope has a divide at $x = 0$ and a lower boundary (the base of the hillslope) at $x = \lambda$.

3.2. Denudation Rates

[23] Soil produced on the hillslope must be removed by some combination of mechanical and chemical denudation (equation (16)). This can be measured as denudation rates,
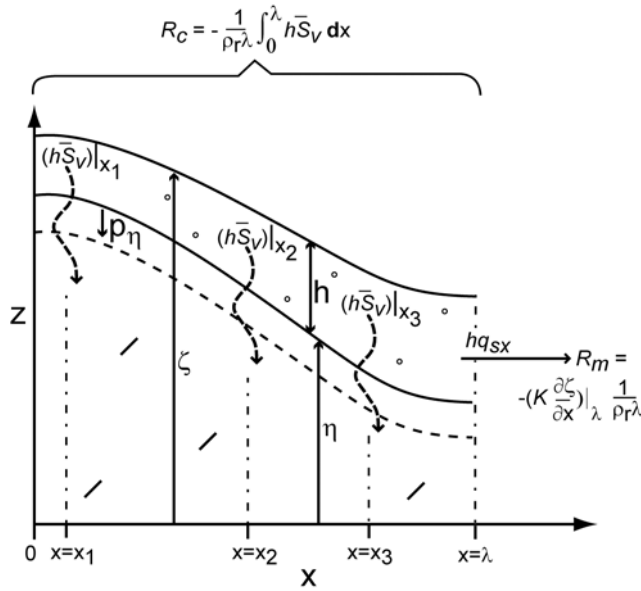
Figure 4. Diagram of denudation balance. A linear sediment transport law is shown. The quantity $h\bar{S}_v$ varies over the hillslope, so this quantity must be integrated over the hillslope to find the chemical denudation rate.

which represent the rate of landscape lowering due to mechanical and chemical processes.

3.2.1. Mechanical Denudation Rate

[24] The mechanical denudation rate averaged over the hillslope is the rate of lowering caused by mechanical hillslope processes and is related to the mechanical flux through the lower boundary of the hillslope by

$$R_m = -\frac{D\bar{\rho}_s}{\rho_r\lambda}\left(\frac{\partial\zeta}{\partial x}\bigg|_\lambda\right), \qquad (20)$$

where R_m (LT^{-1}) is the slope-averaged mechanical denudation rate and λ (L) is the hillslope length. The quantity in parentheses is the slope at the hillslope base.

3.2.2. Chemical Denudation Rate

[25] The local chemical denudation rate must be integrated over the length hillslope to find the slope-averaged rate because precipitation from or dissolution into the aqueous phase is occurring at all points on the hillslope (Figure 4). The slope-averaged chemical denudation rate R_c (LT^{-1}) is

$$R_c = -\frac{\bar{\rho}_s}{\rho_r\lambda}\int_0^\lambda \frac{h\bar{S}_v}{\bar{\rho}_s}dx. \qquad (21)$$

[26] *Carson and Kirkby* [1972] argue that in humid environments, soil depth h tends to increase away from the divide, and in arid regions the soil thins away from the divide. Recent work [e.g., *Heimsath et al.*, 1997; *Small et al.*, 1999] has shown that soil production is a function of soil depth, so if soil depth varies in space, so will soil production. If soil production is the dominant mechanism driving p_η, then spatially varying soil production will violate the assumption of steady topographic form because the bedrock surface will be lowering at different rates at different points on the hillslope. *Furbish and Fagherazzi* [2001], however, proposed that the soil production function

may vary as a function of distance from the divide. It is assumed here that soil production function does vary with x. This variation is assumed to lead to spatially constant p_η, despite spatial variations in soil depth. The simplest approximation of the soil depth that still can describe whether it is thinning, thickening, or remaining constant as a function of distance from the divide is

$$h = mx + h_0, \qquad (22)$$

where m (dimensionless) is the slope of the soil depth function and h_0 (L) is the soil depth at the divide.

[27] The depth-averaged mass loss rate due to chemical processes must also be described. The spatial and temporal distribution of mineral weathering, particularly in the vadose zone, is still largely unknown and is an area of active research [e.g., *Anderson et al.*, 2002; *Egli et al.*, 2001; *Millot et al.*, 2002; *Sander*, 2002; *Stonestrom et al.*, 1998; *White et al.*, 1999]. A spatially homogenous weathering rate is simply assumed from the onset of the analysis in the work of *Small et al.* [1999]. In this contribution we also assume that the depth-averaged mass loss rate due to chemical processes is spatially uniform over the hillslope, in the interest of simplicity. A more general form of the local lowering rate due to chemical processes is described in Appendix C.

[28] Inserting equation (22) into equation (21) and integrating gives

$$R_c = -\frac{\bar{S}_v}{2\rho_r}(\lambda m + 2h_0). \qquad (23)$$

A ratio between the chemical denudation rate and the total denudation rate may be defined. This ratio, θ_d (dimensionless), is named the denudation ratio:

$$\theta_d = \frac{R_c}{R_c + R_m}. \qquad (24)$$

Equations (16) and (24) can be inserted into equation (23) and solved for $\bar{S}_v$:

$$\bar{S}_v = -\frac{2R_T\theta_d\rho_r}{\lambda m + 2h_0}. \qquad (25)$$

3.3. Curvature, Slope, and Profile of the 1-D Steady State Hillslope

[29] When equations (22) and (25) are inserted into equation (19), an equation for the curvature of the hillslope as a function of distance from the divide may be found:

$$\frac{\partial^2\zeta}{\partial x^2} = ax - b, \qquad (26a)$$

where

$$a = \frac{2R_T\theta_d\rho_r m}{D\bar{\rho}_s(\lambda m + 2h_0)} \qquad (26b)$$

and

$$b = \frac{\rho_r R_T}{D\bar{\rho}_s}\left(1 - \frac{2\theta_d h_0}{\lambda m + 2h_0}\right). \qquad (26c)$$

[30] The local slope and land surface elevation of the hillslope may be determined by applying the appropriate

boundary conditions. The slope at the base may be found by combining equations (20), (23), and (24):

$$\left.\frac{\partial \zeta}{\partial x}\right|_\lambda = -\frac{R_T \rho_r \lambda}{D \bar{\rho}_s}(1 - \theta_d). \tag{27}$$

If the slope at the lower boundary is zero, then there is no mechanical transport out of the system. Such a hillslope could be said to be "disconnected mechanically" from the fluvial system and would have a denudation ratio of one.

[31] By integrating equation (26) and using the above boundary condition (equation (27)), the equation for the slope as a function of distance from the divide is found to be

$$\frac{\partial \zeta}{\partial x} = \frac{ax^2}{2} - bx, \tag{28}$$

where a and b were defined in equations (26b) and (26c). The surface coordinate at the base of the hillslope is chosen to be $\zeta(\lambda) = 0$. Integrating equation (28) gives the equation for the surface of the hillslope:

$$\zeta = \frac{a(x^3 - \lambda^3)}{6} - \frac{b(x^2 - \lambda^2)}{2}. \tag{29}$$

The maximum elevation on the hillslope will be at $x = 0$.

3.4. Features of the 1-D Steady State Hillslope

[32] The curvature of the hillslope is linear with respect to distance from the divide when chemical denudation or deposition is occurring in the hillslope soil. This is a departure from the end-member case, when there is no chemical denudation ($\theta_d = 0$), where the curvature is constant. There are several important features to equation (26). In the end-member case, where there is no chemical denudation ($\theta_d = 0$), the curvature will be constant, and the equation reduces to the familiar equation

$$D\frac{\partial^2 \zeta}{\partial x^2} = -\frac{\rho_r R_T}{\bar{\rho}_s}. \tag{30}$$

If the soil depth is not changing with distance from the divide ($m = 0$), the curvature is again constant but is less than the curvature found in the case of $\theta_d = 0$:

$$D\frac{\partial^2 \zeta}{\partial x^2} = -\frac{\rho_r R_T}{\bar{\rho}_s}(1 - \theta_d). \tag{31}$$

Equation (31) has the important implication that if one measures the sediment diffusivity and estimates the soil production rate without accounting for the chemical denudation, one will underestimate (or overestimate, if there is precipitation of solutes in the soil) the production rate by a factor of $(1 - \theta_d)$.

[33] The curvature at the divide is

$$\left.\frac{\partial^2 \zeta}{\partial x^2}\right|_{x=0} = -\frac{\rho_r R_T}{D\bar{\rho}_s}\left(1 - \frac{2\theta_d h_0}{\lambda m + 2h_0}\right). \tag{32}$$

For the curvature to be negative, or, in other words, for the hillslope to be convex at the divide, the parameters must satisfy the following condition:

$$\frac{2h_0 \theta_d}{\lambda m + 2h_0} < 1. \tag{33}$$

For hillslopes in which there is either net chemical deposition (θ_d is negative), or the soil thins with distance

from the divide (m is negative), or both, there may be concave slopes at the divide. This would mean that the greatest slope would be at the divide. Many hillslopes, however, have soils that thicken away from the divide (m is positive) and net chemical denudation (θ_d is positive), and therefore most hillslopes that are both mechanically and chemically weathering should be convex at the divide. This is the same result as in the case of the hillslope that is denuding through mechanical means only and is the typical morphology of natural hillslopes in humid climates.

[34] If curvature is a linear function of distance from the divide, it is possible that there will be a point some distance from the divide where curvature equals zero and the hillslope transitions from negative to positive curvature or vice versa. This point separates the convex portion of the hillslope from the concave portion of the hillslope. Setting the curvature equal to zero in equation (26), the location of this inflection point ξ (L) may be calculated:

$$\xi = \frac{m\lambda + 2h_0(1 - \theta_d)}{2m\theta_d}. \tag{34}$$

There is no inflection point on hillslopes with $\xi > \lambda$ because the predicted location of the inflection point lies farther from the divide than the hillslope base. Such hillslopes will be only concave or convex. When $0 < \xi < \lambda$, the hillslope is convex-concave. The condition for a convex-concave slope may be stated as

$$\frac{m\lambda + 2h_0}{2m\lambda + 2h_0} < \theta_d. \tag{35}$$

If $2h_0 \gg m\lambda$, then θ_d will approach unity, and a convex-concave slope may only be maintained at steady state if all denudation is occurring through the mechanism of chemical weathering. If $2h_0 \ll m\lambda$, then θ_d approaches 0.5. Thus the chemical denudation rate must be at least as great as the mechanical denudation rate if a convex-concave slope is to exist at steady state.

[35] If the hillslope has a convex-concave form, the slope with the maximum absolute value (S_{max}) will occur at the inflection point. This slope is

$$S_{max} = \left| -\left(\frac{R_T \rho_r}{D\bar{\rho}_s}\right)\frac{[2h_0(1 - \theta_d) + m\lambda]^2}{4\theta_d m(m\lambda + 2h_0)} \right|. \tag{36}$$

3.5. Nondimensionalization

[36] In the analysis of sections 3.1–3.4, important quantities such as the shape of the hillslope ($\zeta(x)$), the maximum slope, the inflection point, and the curvature are described in terms of several parameters. These relationships can be collapsed into relationships between a smaller number of parameters through nondimensionalization. All terms that have dimension length may be scaled by the hillslope length λ:

$$\zeta_* = \frac{\zeta}{\lambda}, \quad \eta_* = \frac{\eta}{\lambda}, \quad x_* = \frac{x}{\lambda},$$
$$\xi_* = \frac{\xi}{\lambda}, \quad h_* = \frac{h_0}{\lambda}, \tag{37}$$

where the asterisk indicates a dimensionless quantity. Two timescales may also be identified. The first is the mean residence time of a particle on the hillslope (T_R (T)), which is the average depth of the soil on the hillslope ($\langle h \rangle$ (L)) divided by the total denudation rate:

$$\langle h \rangle = \frac{1}{\lambda} \int_0^{\lambda} (h_0 + mx)dx = h_0 + \frac{m\lambda}{2} \qquad (38)$$

$$T_R = \frac{\langle h \rangle}{R_T}. \qquad (39)$$

Another timescale is the relaxation timescale. *Fernandes and Dietrich* [1997] and *Roering et al.* [2001] explored this numerically, but here we use the analytical relaxation timescale that is commonly seen in the analysis of heat and chemical diffusion as well as in the work of *Furbish and Fagherazzi* [2001], *Jyotsna and Haff* [1997], and *Koons* [1989]:

$$T_D = \frac{\lambda^2}{D}. \qquad (40)$$

The "diffusive" timescale T_D (T) is the square of the system size (in this case the hillslope length) times the inverse of its diffusivity (which is a measure of the effectiveness of the transport process). A nondimensional ratio may be defined that is the ratio of the residence timescale to the diffusive timescale:

$$\theta_T = \frac{T_R}{T_D}. \qquad (41)$$

This ratio will be called the transport ratio as it is a proxy for the ratio of sediment entering the active layer to the sediment transported through diffusion-like mechanical processes. If no other parameters change, increasing the total denudation rate will result in a smaller value of θ_T, whereas increasing the diffusivity of the hillslope will increase θ_T.

[37] Finally, a density ratio may be formed:

$$\tau_d = \frac{\bar{\rho}_s}{\rho_r}. \qquad (42)$$

[38] Important quantities may now be recast in nondimensional terms. The nondimensional inflection point is

$$\xi_* = \frac{m - 2h_*(\theta_d - 1)}{2m\theta_d}. \qquad (43)$$

The maximum slope as a function of nondimensional parameters is

$$S_{max} = \frac{\left[m - 2h_*(\theta_d - 1)\right]^2}{8m\theta_d\theta_T\tau_d}. \qquad (44)$$

The equation for the nondimensional hillslope profile is

$$\zeta_* = \frac{a_*\left(x_*^3 - 1\right)}{6} - \frac{b_*\left(x_*^3 - 1\right)}{2}, \qquad (45a)$$

where

$$a_* = \frac{\theta_d m}{\theta_T \tau_d} \qquad (45b)$$

and

$$b_* = \frac{m + 2h_*(1 - \theta_d)}{2\theta_T \tau_d}. \qquad (45c)$$

4. Discussion

### 4.1. Effect of Chemical Weathering on the Morphology of Steady State Hillslopes

[39] In the end-member case, when both m and θ_d equal zero, the hillslope profile will be parabolic and the curvature will be uniform, as predicted qualitatively by *Gilbert* [1909]. This end-member hillslope morphology may be compared with the morphology of hillslopes that experience chemical weathering in the soil. Figure 5 shows morphologies of hillslopes with varying denudation ratios and m values. If all other parameters are constant, increasing denudation ratios lead to gentler slopes and less relief. The hillslopes that have chemical weathering diverge from the parabolic shape of the end-member case ($m = 0$, $\theta_d = 0$); for hillslopes with spatially homogenous $\bar{S}_v$ and finite m values the curvature increases linearly as a function from the divide. The increase is due to the linear increase in the local lowering rate due to chemical denudation as a function of distance from the divide, which is a result of the assumptions used in the development of the governing equations. Appendix C addresses the possibility of nonlinearities in the local soil lowering rate due to chemical processes as a function of distance from the divide. If $m = 0$ and θ_d is nonzero, hillslope curvature will be constant and the profile will be parabolic as in the end-member case of no chemical denudation, but the presence of chemical denudation will reduce the relief and will lead to gentler slopes than in the purely mechanical case.

4.2. Conceptual Explanation of the Steady State Convex-Concave Hillslope

[40] Figure 6 shows the relationship between sediment entering the active layer and sediment transport and removal due to the two denudation mechanisms. If the total amount of sediment dissolved chemically upslope of a point is increasing less than the total amount of sediment entering the active layer, then the amount of sediment that must be transported mechanically is increasing at that point, and therefore the hillslope will be steepening away from the divide. If, however, the denudation ratio is >0.5, at some point on the slope the amount of sediment denuded chemically will be increasing faster than the amount of sediment entering the active layer from upslope. Downslope of this point the sediment transported mechanically must decrease in the downslope direction, and the slope will become gentler, giving concave topography.

4.3. Conditions for Steady State Hillslopes With Convex-Concave Profiles

[41] Equation (43) may be used to predict the combinations of dimensionless soil depth at the divide (h_*), the rate of increase in soil depth away from the divide (m), and the denudation ratio (θ_d) that occur on steady state hillslopes with convex-concave profiles. The parameter values of a hillslope with an inflection point at the base of the hillslope
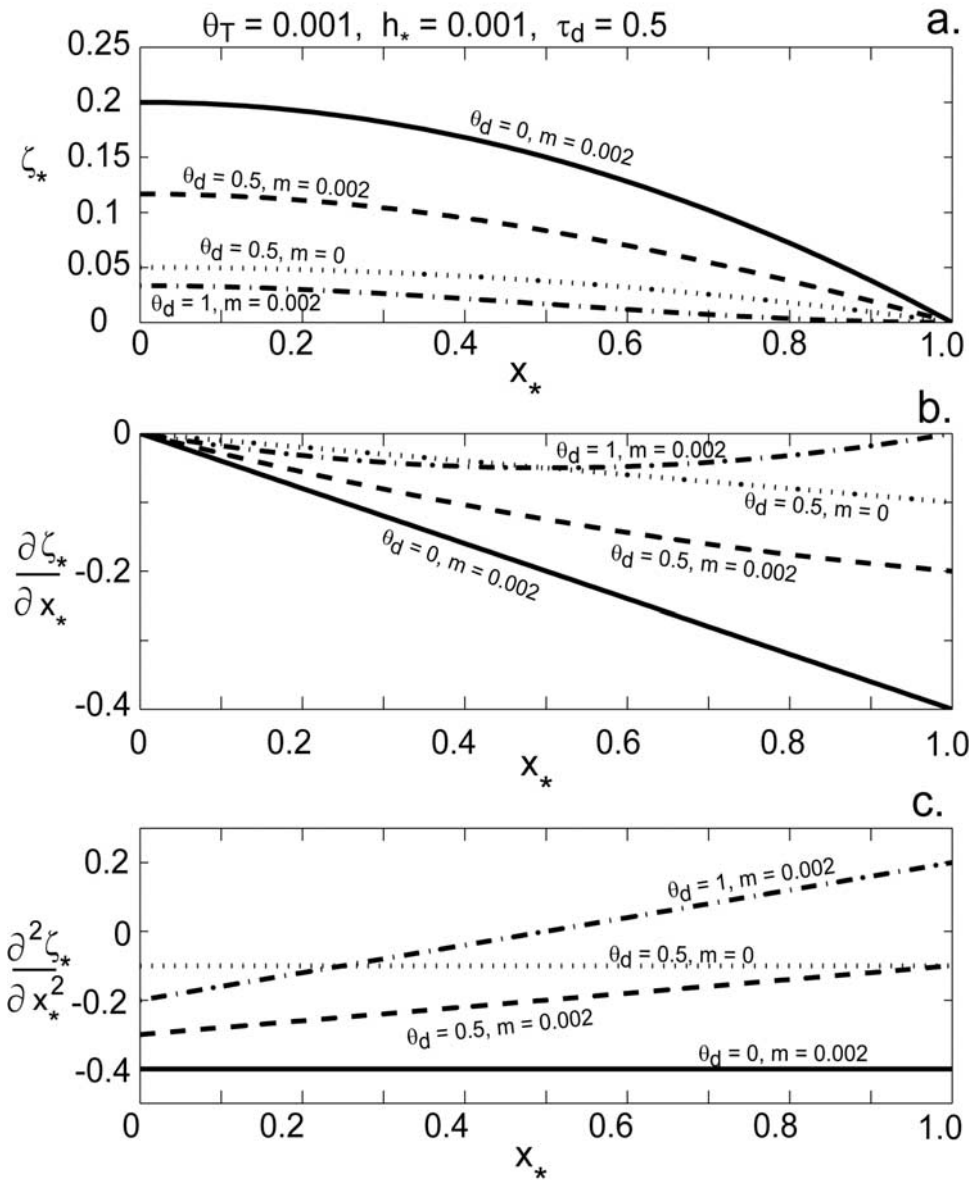
Figure 5. Nondimensional (a) surface elevation, (b) slope, and (c) curvature for hillslopes with varying parameter values.

can be represented as a surface. Two such surfaces are shown in Figure 7. The surface in Figure 7a represents the parameter values at which the inflection point is at the base of the hillslope. Parameter values plotting below this surface have convex-concave profiles at steady state. Hillslopes that have higher denudation ratios and for which soil depth increases faster away from the divide are favored to have convex-concave slope profiles. Smaller values of the dimensionless soil depth at the divide, h_*, also favor convex-concave slope profile. Thus hillslopes with shallower soils at the divide and longer slope lengths are more likely to have convex-concave profiles at steady state. As noted by inspection of equation (35), the value of the denudation ratio must be >0.5 for a convex-concave slope to exist. A hillslope with $\theta_d = 1$, or, in other words, a hillslope in which all the denudation is occurring through chemical means, always has a convex-concave profile, and the inflection

points of these hillslopes are located halfway between the divide and the outlet ($\xi = \lambda/2$). Mechanical sediment transport still functions on these hillslopes, and particles entrained from the bedrock at and away from the divide still move downslope, but the slope at the hillslope outlet is zero, so the horizontal mechanical sediment transport there must be zero, and all mass converted to soil from the underlying bedrock is removed through chemical means as it moves toward the base of the hillslope.

4.4. Transport Ratios for Steady State Hillslopes With Convex-Concave Profiles

[42] We may assume that in many landscapes, climate and tectonics combine to form an initial drainage network. If these conditions then change, causing the drainage network to retreat (that is, to decrease the drainage density or reduce the total length of the channels in the fluvial system), the

now unchanneled valleys will begin to fill with sediment. At some time after the retreat of the drainage network, the unchanneled valleys may relax to a steady state convex-concave shape. In this situation the antecedent drainage network has set the length of the hillslopes. The climatic and tectonic regime that lead to the steady state unchanneled valleys are also external influences that help to set the shape of the hillslope. These external influences are contained within the transport ratio θ_T along with the depth of the soil at the divide and the soil depth increase away from the divide (m), which are set by hillslope processes. For a range of maximum slopes (S_{max}, or the slope at the inflection point) and m values the transport ratio can vary over several orders of magnitude. The predicted transport ratios (see Figure 8) may be compared to physically realistic θ_T values.

4.5. Comparison of Theoretical Transport Ratios With Transport Ratios Calculated From Field Data

[43] Physically realistic ranges of the transport ratio may be obtained from measured values for diffusivities, total denudation rates, hillslope length scales, and reasonable soil parameters (Figure 8). The relatively small number of field studies of hillslope diffusivities have reported values of D ranging from order 10^{-4} to order 10^{-1} m^2 yr^{-1} [see *Fernandes and Dietrich*, 1997, Table 1]. More humid regions will typically have higher values of D, although D also depends on the biota, the temperature, and the nature of sediment in a given landscape [*Anderson*, 2002].

[44] The upper range on exhumation rate is 1.0×10^{-2} m yr^{-1} [*Burbank*, 2002], but the most rapid documented chemical denudation rate is 5.8×10^{-5} m yr^{-1} [*White et al.*, 1998]. Exhumation must balance denudation at steady state. Because the mechanical denudation rate must be less than the chemical denudation rate in order for a convex-concave slope to be in steady state, the upper limit on total denudation rate that allows this hillslope form is $\sim 10^{-4}$ m yr^{-1}. Such a denudation rate, although several orders of magnitude lower than the fastest known denudation rates, is nevertheless a rate of denudation that is representative of areas of active tectonics. The Oregon Coast Range near the experimental site of *Anderson et al.* [2002] has been estimated to have a long-term uplift rate (which should be similar to the total denudation rate at steady state) of 10^{-4} m yr^{-1}. The lowest denudation rate is (trivially) zero, but as a point of reference, the time-averaged uplift due to tectonic flexure on the Atlantic margin of the United States is estimated to be $2 \times 10^{-6} – 1 \times 10^{-5}$ m yr^{-1} [*Pazzaglia and Gardner*, 1994].

[45] Hillslopes are typically tens to hundreds of meters long. Soil depth can be zero, but the upper limit of soil depth is harder to quantify. As researchers in the Amazon basin have found rooting depths of 8 m [*Nepstad et al.*, 1994], and root growth causes mechanical disturbance of the soil [e.g., *Gabet et al.*, 2003], it is presumed that the upper limit on soil depths is on the order of 10 m.

[46] With this information, physically meaningful values may be established for T_R, T_D, and θ_T. For a very deep soil and a total denudation rate similar to the estimated uplift rate of the Atlantic margin of the United States, T_R will be on the order of 10^8 years. Low hillslope lengths and high diffusivities give a T_D of order 10^3 years and a θ_T of order 10^5. This value is several orders of magnitude larger than
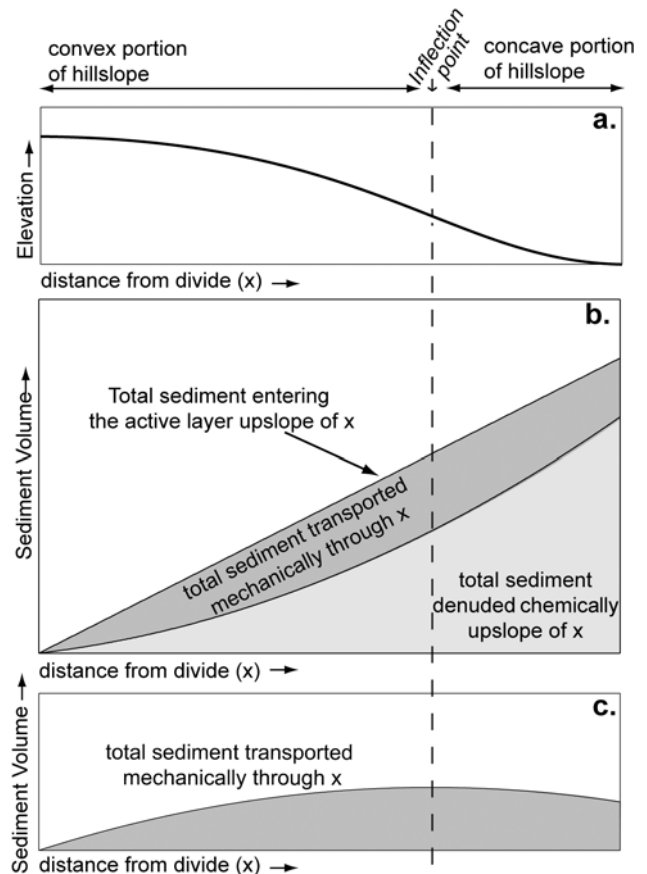
Figure 6. (a) Diagram of a convex-concave slope and the denudation balance as a function of distance from the divide. (b) The total sediment denuded chemically is a nonlinear function of the distance from the divide. (c) Below the inflection point the total amount of sediment denuded chemically above x begins to increase more quickly than the corresponding increase in total sediment entering the active layer upslope, and the sediment that must pass through x mechanically decreases with increasing distance from the divide.

the highest values calculated for θ_T in Figure 8. Therefore the end-member combination of the residence and relaxation time will not have convex-concave slopes at steady state. In landscapes with low total denudation and thick soils, hillslopes must either be longer or have lower diffusivities than the end-member hillslopes in order to have steady state convex-concave slopes. With a hillslope length of order 10^3 m and a diffusivity of 10^{-2} m^2 yr^{-1} the T_D value will be of order 10^8 years, and θ_T will be of order unity. This is in the range of θ_T values predicted in Figure 8 for slopes of low relief. Lowlands are, by definition, low-relief landscapes. Steady state convex-concave hillslopes of higher relief will have thinner soils, lower diffusivities, shorter slopes, and faster total denudation rates. For example, a hillslope with a total denudation rate of order 10^{-4} m yr^{-1}, a diffusivity of order 10^{-3} m^2 yr^{-1}, an average soil depth of order 1 m, and a length of order 100 m will have a θ_T value of 10^{-3}. Table 1 shows the values of θ_T for selected combinations of naturally occurring soil depths, uplift rates, diffusivities, and hillslope lengths.
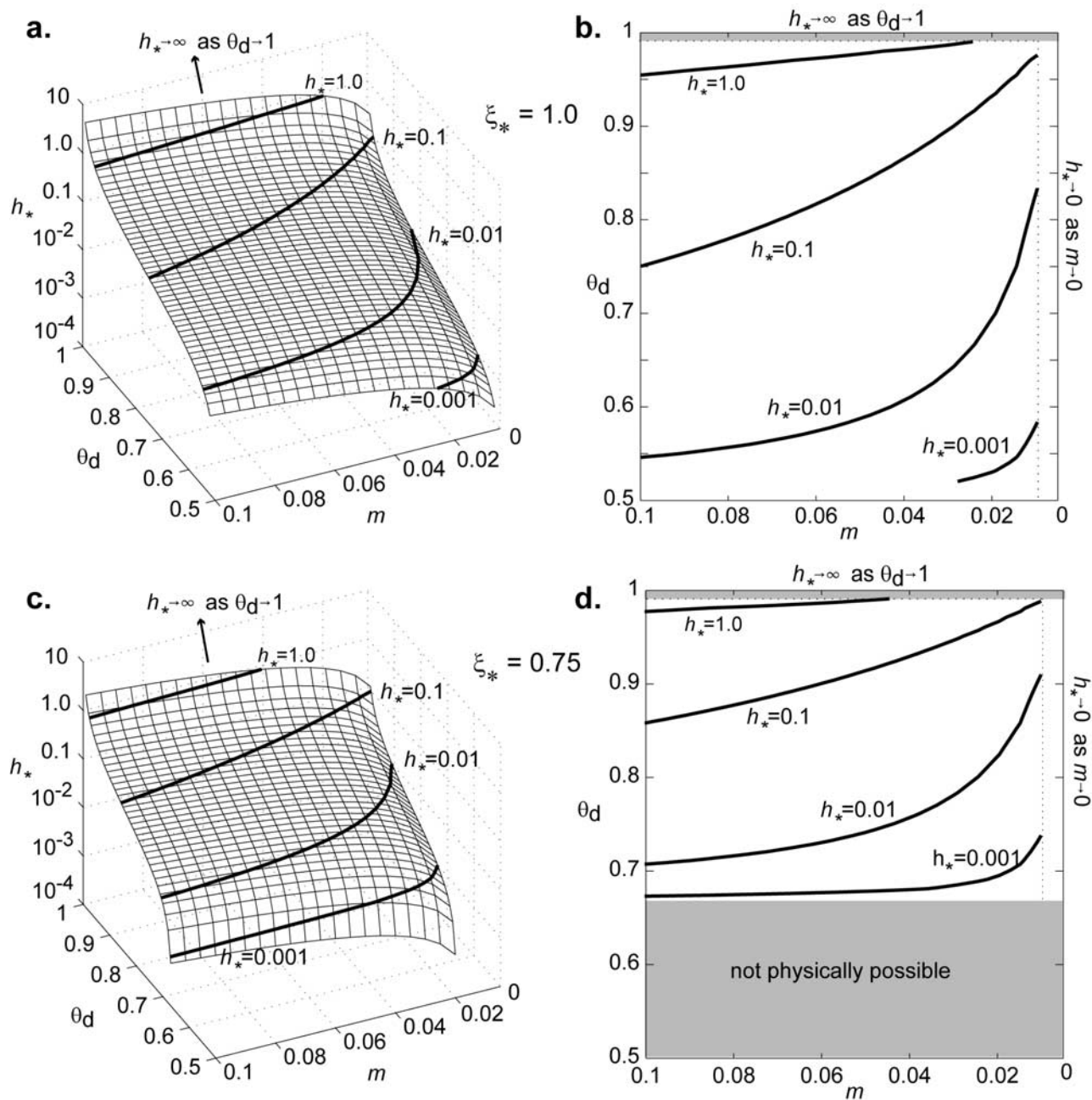
Figure 7. Dimensionless depth of soil at the divide (h_*) for (a, b) hillslopes with an inflection point at the hillslope outlet ($x = \lambda$) and (c, d) hillslopes with an inflection point three quarters of the length of the hillslope from the divide. Surfaces (Figures 7a and 7c) and contour plots (Figures 7b and 7d) are shown. Any hillslope with a combination of h_*, denudation ratio (θ_d), and rate of the increase of soil depth away from the divide (m) that plots below the surface in Figure 7a has a convex-concave slope.

[47] Some representative hillslope profiles are plotted in Figure 9. These hillslopes range from high relief (Figure 9a), to moderate relief (Figures 9b and 9c), to low relief (Figure 9d). As shown in Figure 9, hillslopes with a wide range of parameter values may have convex-concave profiles at steady state.

4.6. Occurrence of Hillslopes With Denudation Ratios >0.5

[48] It is required that $\theta_d > 0.5$ for the existence of steady state hillslopes with convex-concave profiles. Is this condi-

tion physically realistic? In studies of river basin denudation rates, *Summerfeld and Hulton* [1994] and *Gaillardet et al.* [1997] found denudation ratios of 0.5 or greater (see Table 2). As stated earlier, the highest measured chemical denudation rate is on the order of 10^{-4} m yr^{-1}. As local erosion rates can be several orders of magnitude greater than the fastest measured chemical denudation rate, if a basin includes one or more subbasins that are undergoing rapid physical erosion, this will skew the basin-averaged denudation ratio in favor of mechanical erosion. We also note that chemical denudation rates calculated by solute fluxes incorporate dissolution that
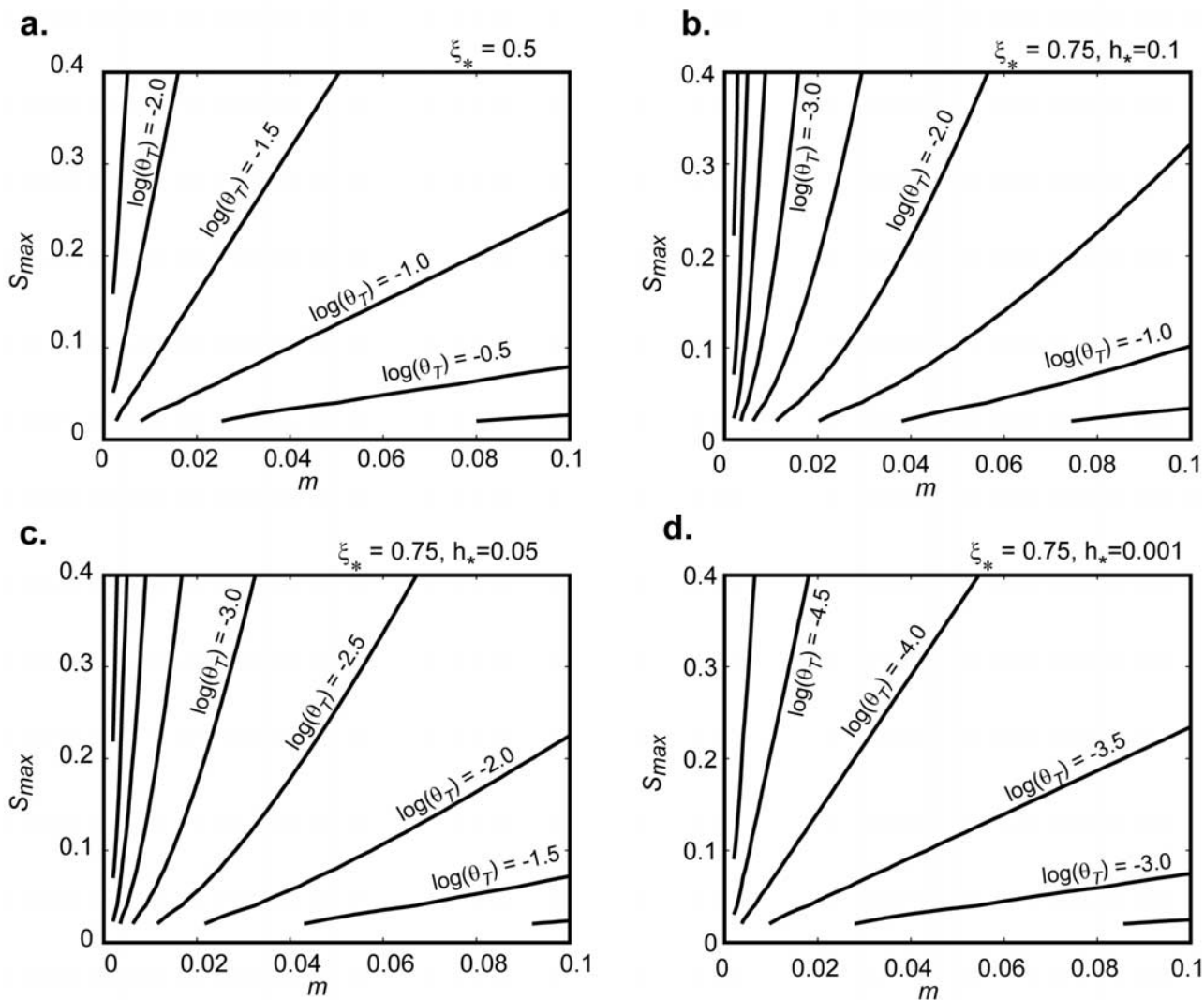
Figure 8. Contour plot of the transport ratio θ_T for an inflection point of (a) $\xi_* = 0.5$ and (b–d) $\xi_* = 0.75$ and dimensionless soil depth $h_* = 0.1$ (Figure 8b), $h_* = 0.05$ (Figure 8c), and $h_* = 0.001$ (Figure 8d). The density ratio τ_d for these plots is 0.5.

occurs in both bedrock and the soil mantle. Nonetheless, *Anderson et al.* [2002] found that chemical weathering is more vigorous in soil than in bedrock due to the fact that more water may flush the soil due to its higher porosity and because minerals in the soil have larger available surface area for reactions to occur.

5. Conclusions

[49] Chemical denudation can affect the curvature, slope, and profile of hillslopes. Downslope changes in soil lowering due to chemical processes will be reflected in the hillslope morphology, leading to hillslopes that have different relief, slope, and shape (e.g., nonparabolic) than hillslopes undergoing only diffusion-like sediment transport. We have shown that hillslopes under certain conditions may have a convex-concave profile at steady state. This is in contrast to slopes only experiencing diffusion-like mechanical sediment transport, wherein only slopes that are transient and are storing sediment at their base may have a convex-concave profile. Hillslopes with a variety of lengths,

soil depths, variations in soil depth as a function of distance from the divide, total denudation rates, sediment diffusivities, and density changes as soil is converted to bedrock may have a convex-concave profile. An important condition for the existence of a hillslope with a convex-concave profile at steady state is that the chemical denudation rate must exceed the mechanical denudation rate on the hillslope. Although there is evidence that chemical denudation is greater than physical denudation in some large river

Table 1. Values of the Transport Ratio (θ_T) For Naturally Occurring Rates of Total Denudation (R_T), Average Soil Depth ($\langle h \rangle$), Hillslope Length (λ), and Sediment Diffusivity (D)[a]

θ_T	R_T, m yr^{-1}	$\langle h \rangle$, m	λ, m	D, m^2 yr^{-1}	Convex-Concave Profile Possible?
6.25×10^2	2×10^{-6}	5	20	10^{-1}	no
10^{-2}	5×10^{-6}	5	500	10^{-3}	yes
10^{-4}	10^{-4}	1	100	10^{-3}	yes

[a]Note that these values are slightly different than the end-member values and have been chosen because they are presumably representative of a larger number of natural hillslopes.
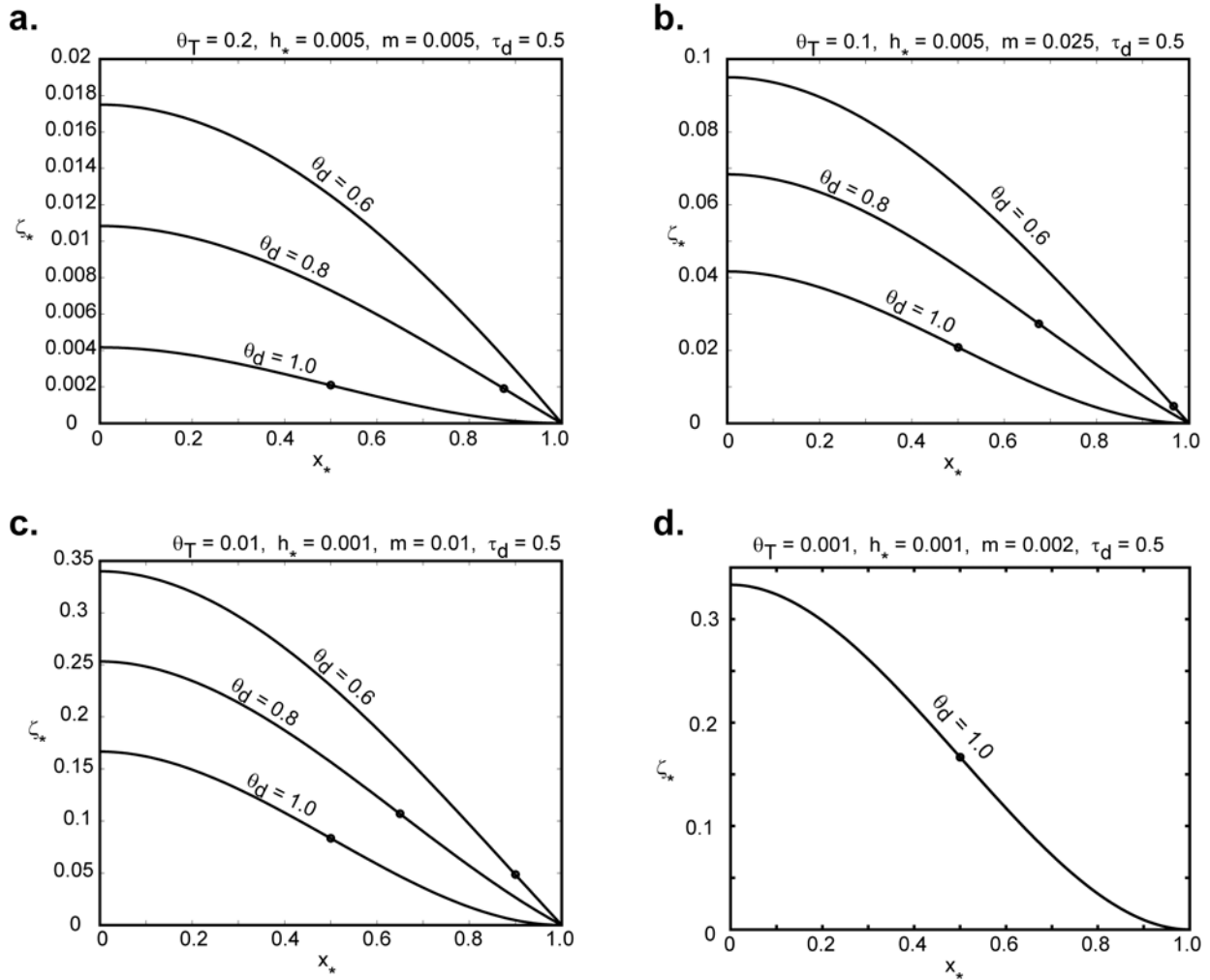
Figure 9. Hillslope profiles for various values of the transport ratio θ_T, dimensionless soil depth at the divide (h_*), rate of increase in soil depth away from the divide (m), and denudation ratio (θ_d). The value of the density ratio τ_d is 0.5 for all plots. Note the change in vertical scale. Black dots indicate the inflection point (transition from negative to positive curvature). The curve in Figure 9a without a black dot has a predicted inflection point at $x_* > 1$.

basins, further work is required to quantify both mechanical and chemical denudation rates at the hillslope scale. It will be important at this scale to measure the chemical denudation that occurs in the soil as dissolution in the bedrock does not directly affect the hillslope topography. Chemical weathering in soils is an area of active research, but the spatial variation in the local rate of soil lowering due to chemical processes at the hillslope is not well understood. Further research in this area is needed in order to better understand the impact of chemical weathering on hillslope morphology.

Appendix A

[50] The mean value theorem may be stated as, for example,

$$\bar{f} = \frac{1}{\zeta - \eta} \int_{\eta}^{\zeta} f(x,y,z,t)dz = \frac{1}{h} \int_{\eta}^{\zeta} f(x,y,z,t)dz, \qquad (A1)$$

where the overbar denotes a depth-averaged quantity and f is some function of position (x, y, and z) and time (t). Leibniz's rule may be stated as

$$\int_{\eta(x,y,t)}^{\zeta(x,y,t)} \frac{\partial}{\partial x} f(x,y,z,t)dz = \frac{\partial}{\partial x} \int_{\eta(x,y,t)}^{\zeta(x,y,t)} f(x,y,z,t)dz$$
$$-f(\zeta(x,y,t),x,y,t)\frac{\partial \zeta}{\partial x}$$
$$+f(\eta(x,y,t),x,y,t)\frac{\partial \eta}{\partial x}. \qquad (A2)$$

Appendix B

[51] Equation (13) allows one to track changes in the soil depth h. In some cases, it may be more desirable to track the change in surface elevation ζ. One method yielding a relatively simple equation is carried out by multiplying

Table 2. Denudation Ratios (θ_d) From Selected River Basins

θ_d	River Basin	Location
0.857	Dnepr[a]	Ukraine, Belarus, Russia
0.759	Lena[a]	Russia
0.647	Ob[a]	Russia
0.944	St. Lawrence[a]	Canada
0.783	Yenisei[a]	Russia
0.5	Urucara (Amazon subbasin)[b]	Brazil
0.5	Tapajos (Amazon subbasin)[b]	Brazil

[a]From *Summerfeld and Hulton* [1994].
[b]From *Gaillardet et al.* [1997].

equation (8) by the depth-averaged dry bulk soil density (and with the assumption of no horizontal tectonic velocities):

$$\bar{\rho}_s \frac{\partial \eta}{\partial t} - \bar{\rho}_s U_z|_\eta + \bar{\rho}_s p_\eta = 0. \tag{B1}$$

Because the terms to the left of the equality in equation (B1) equal zero, these terms may be added to equation (13). Equation (6) is also inserted into the unsteady term in equation (13) such that the soil depth h in this term is cast in terms of ζ and η. The chain rule is then used to arrive at

$$\bar{\rho}_s \frac{\partial \zeta}{\partial t} + h \frac{\partial \bar{\rho}_s}{\partial t} + \nabla_2 \cdot (h\mathbf{q_s}) - h\bar{S}_v - (\rho_r - \bar{\rho}_s)p_\eta - \bar{\rho}_s U_z = 0 \tag{B2}$$

or, in component form,

$$\bar{\rho}_s \frac{\partial \zeta}{\partial t} + h \frac{\partial \bar{\rho}_s}{\partial t} + \frac{\partial}{\partial x}(hq_{sx}) + \frac{\partial}{\partial y}(hq_{sy}) = h\bar{S}_v + (\rho_r - \bar{\rho}_s)p_\eta + \bar{\rho}_s U_z. \tag{B3}$$

Appendix C

[52] Equation (24) contains three terms which are local rates of soil surface lowering due to mechanical sediment transport, chemical denudation, and total denudation (which has replaced soil production due to the steady state assumptions). By assuming spatial homogeneity of $\bar{S}_v$ and a linear increase in soil depth away from the divide the local rate of soil lowering due to chemical weathering, r_c ($L\ T^{-1}$) was cast as a linear function of distance from the divide:

$$r_c = \frac{h\bar{S}_v}{\bar{\rho}_s} = \frac{(mx + h_0)\bar{S}_v}{\bar{\rho}_s}. \tag{C1}$$

A more general formulation could simply treat the local rate of soil lowering due to chemical weathering as a power law function of x:

$$r_c = \alpha x^\beta + r_0, \tag{C2}$$

where α and β are empirical coefficients and r_0 is the local rate of soil lowering due to chemical weathering at the divide. If $\beta = 1$, then equation (C2) reduces to equation (C1), where

$$r_0 = \frac{h_0 \bar{S}_v}{\bar{\rho}_s} \tag{C3a}$$

$$\alpha = \frac{m\bar{S}_v}{\bar{\rho}_s}. \tag{C3b}$$

The chemical denudation rate may be calculated by integrating the local chemical denudation rate, as done in equation (26). This gives

$$R_c = -\frac{\bar{\rho}_s}{\rho_r}\left(\frac{\alpha x^\beta}{1 + \beta} + r_0\right). \tag{C4}$$

Equation (29) may be inserted into equation (C4), which may then be solved for r_0:

$$r_0 = -\frac{\bar{\rho}_s}{\rho_r}R_T\theta_d - \frac{\alpha\lambda^\beta}{1 + \beta}. \tag{C5}$$

Inserting equations (C5) and (C2) into equation (24) gives the hillslope curvature:

$$\frac{\partial^2 \zeta}{\partial x^2} = \frac{\alpha}{D}x^\beta + \frac{1}{D}\left(\frac{\rho_r}{\bar{\rho}_s}R_T(1 - \theta_D) - \frac{\alpha\lambda^\beta}{1 + \beta}\right). \tag{C6}$$

If the increase or decrease in r_0 as a function of distance from the divide is nonlinear, so too will be the curvature. The empirical coefficients α and β may depend on many factors, including, but not limited to, climate, hydrology, and the kinetics of chemical reactions within the soil and are a significant control on hillslope morphology. Recent studies have begun to explore spatial variations in chemical weathering at the hillslope scale [e.g., *Green et al.*, 2003]; such studies may be used in the future to better parameterize equation (C2).

Notation

α	empirical coefficient for power law description of soil surface lowering due to chemical weathering as a function of x.
β	empirical exponent for power law description of soil surface lowering due to chemical weathering as a function of x.
D	sediment diffusivity ($L^2 T^{-1}$).
d_ζ	deposition or erosion at surface of soil ($L T^{-1}$).
η	coordinate of the bedrock-soil interface (L).
η_*	dimensionless bedrock-soil interface coordinate.
η_{bl}	elevation of soil-bedrock boundary with respect to base level (L).
η_λ	base-level elevation (L).
h	soil depth (L).
$\langle h \rangle$	average depth of soil over a hillslope (L).
h_0	depth of soil at hillslope divide (L).
K	sediment diffusion coefficient ($M L^{-1} T^{-1}$).
λ	hillslope length (L).
m	slope of soil depth as a function of distance from divide (dimensionless).
p_η	rate of change of the elevation of the soil-bedrock boundary under conditions of no tectonic velocities ($L T^{-1}$).
$\mathbf{q}_s$	sediment flux vector ($M L^{-2} T^{-1}$).
q_{sx}, q_{sy}	components of sediment flux vector in the x and y directions, respectively ($M L^{-2} T^{-1}$).
ρ_s	dry bulk density of soil ($M L^{-3}$).
$\bar{\rho}_s$	depth-averaged dry bulk density of soil ($M L^{-3}$).
ρ_r	dry bulk density of the material at the soil-bedrock boundary ($M L^{-3}$).

r_c local rate of soil surface lowering due to chemical weathering (LT^{-1}).

r_0 value of r_c at the divide (LT^{-1}).

R_m mechanical denudation rate (LT^{-1}).

R_s chemical denudation rate (LT^{-1}).

R_T total denudation rate (LT^{-1}).

S_{max} absolute value of maximum slope (dimensionless).

S_v chemical denudation and deposition $(ML^{-3}T^{-1})$.

$\bar{S}_v$ depth-averaged chemical denudation and deposition $(ML^{-3}T^{-1})$.

T_R relaxation timescale (T).

T_D diffusive timescale (T).

θ_d denudation ratio (dimensionless).

θ_T transport ratio (dimensionless).

τ_d density ratio (dimensionless).

$\mathbf{U}$ tectonic velocity vector (LT^{-1}).

U_x, U_y, U_z components of the tectonic velocity vector in the x, y, and z directions (LT^{-1}).

$\mathbf{v}_s$ sediment velocity vector (LT^{-1}).

v_{sx}, v_{sy}, v_{sz} components of sediment velocity vector in the x, y, and z directions (LT^{-1}).

$\bar{v}_{sx}, \bar{v}_{sy}, \bar{v}_{sz}$ depth-averaged components of the sediment velocity vector in the x, y, and z directions, respectively (LT^{-1}).

ζ coordinate of the soil surface (L).

ζ_{bl} coordinate of the soil surface relative to base level (L).

ζ_* dimensionless soil surface coordinate.

ξ location of hillslope inflection point (point of zero curvature) (L).

ξ_* location of inflection point (dimensionless).

References

Ahnert, F. (1976), Brief description of a comprehensive three-dimensional process-response model of landform development, *Z. Geomorphol.*, 25, 29–49.

Ahnert, F. (1987), Approaches to dynamic equilibrium in theoretical simulations of slope development, *Earth Surf. Processes Landforms*, 12(1), 3–15.

Anderson, R. S. (1994), Evolution of the Santa Cruz Mountains, California, through tectonic growth and geomorphic decay, *J. Geophys. Res.*, 99(B10), 20,161–20,179.

Anderson, R. S. (2002), Modeling the tor-dotted crests, bedrock edges, and parabolic profiles of high alpine surfaces of the Wind River Range, Wyoming, *Geomorphology*, 46(1–2), 35–58.

Anderson, S. P., and W. E. Dietrich (2001), Chemical weathering and runoff chemistry in a steep headwater catchment, *Hydrol. Processes*, 15(10), 1791–1815.

Anderson, S. P., W. E. Dietrich, and G. H. Brimhall (2002), Weathering profiles, mass-balance analysis, and rates of solute loss: Linkages between weathering and erosion in a small, steep catchment, *Geol. Soc. Am. Bull.*, 114(9), 1143–1158.

Andrews, D. J., and R. C. Bucknam (1987), Fitting degradation of shoreline scarps by a nonlinear diffusion model, *J. Geophys. Res.*, 92(B12), 12,857–12,867.

Armstrong, A. C. (1976), A three-dimensional simulation of slope forms, *Z. Geomorphol.*, 25, 20–28.

Armstrong, A. C. (1980), Simulated slope development sequences in a 3-dimensional context, *Earth Surf. Processes Landforms*, 5(3), 265–270.

Armstrong, A. C. (1987), Slopes, boundary-conditions, and the development of convexo-concave forms—Some numerical experiments, *Earth Surf. Processes Landforms*, 12(1), 17–30.

Arrowsmith, J. R., D. D. Pollard, and D. D. Rhodes (1996), Hillslope development in areas of active tectonics, *J. Geophys. Res.*, 101(B3), 6255–6275.

Braun, J., and M. Sambridge (1997), Modelling landscape evolution on geological time scales: A new method based on irregular spatial discretization, *Basin Res.*, 9(1), 27–52.

Braun, J., A. M. Heimsath, and J. Chappell (2001), Sediment transport mechanisms on soil-mantled hillslopes, *Geology*, 29(8), 683–686.

Brimhall, G. H., O. A. Chadwick, C. J. Lewis, W. Compston, I. S. Williams, K. J. Danti, W. E. Dietrich, M. E. Power, D. Hendricks, and J. Bratt (1992), Deformational mass-transport and invasive processes in soil evolution, *Science*, 255(5045), 695–702.

Burbank, D. W. (2002), Rates of erosion and their implications for exhumation, *Mineral. Mag.*, 66(1), 25–52.

Carson, M. A., and M. J. Kirkby (1972), *Hillslope Form and Process*, 475 pp., Cambridge Univ. Press, New York.

Culling, W. E. H. (1960), Analytical theory of erosion, *J. Geol.*, 68(3), 336–344.

Davis, W. M. (1889), The rivers and valleys of Pennsylvania, *Natl. Geogr. Mag.*, 1, 183–253.

Dunne, T. (1991), Stochastic aspects of the relations between climate, hydrology, and landform evolution, *Trans. Jpn. Geomorphol. Union*, 12(1), 1–24.

Egli, M., P. Fitze, and A. Mirabella (2001), Weathering and evolution of soils formed on granitic, glacial deposits: Results from chronosequences of Swiss alpine environments, *Catena*, 45(1), 19–47.

Ellis, M. A., A. L. Densmore, and R. S. Anderson (1999), Development of mountainous topography in the Basin Ranges, USA, *Basin Res.*, 11(1), 21–41.

Fernandes, N. F., and W. E. Dietrich (1997), Hillslope evolution by diffusive processes: The timescale for equilibrium adjustments, *Water Resour. Res.*, 33(6), 1307–1318.

Fourier, J. B. (1822), *Theorie Analytique de la Chaleur* (*The Analytical Theory of Heat*) (in French), Didot, Paris. (English translation by A. Freeman, Cambridge Univ. Press, New York, 1878.)

Furbish, D. J., and S. Fagherazzi (2001), Stability of creeping soil and implications for hillslope evolution, *Water Resour. Res.*, 37(10), 2607–2618.

Gabet, E. J. (2000), Gopher bioturbation: Field evidence for non-linear hillslope diffusion, *Earth Surf. Processes Landforms*, 25(13), 1419–1428.

Gabet, E. J. (2003), Sediment transport by dry ravel, *J. Geophys. Res.*, 108(B1), 2049, doi:10.1029/2001JB001686.

Gabet, E. J., O. J. Reichman, and E. W. Seabloom (2003), The effects of bioturbation on soil processes and sediment transport, *Annu. Rev. Earth Planet. Sci.*, 31, 249–273.

Gaillardet, J., B. Dupre, C. J. Allegre, and P. Negrel (1997), Chemical and physical denudation in the Amazon River basin, *Chem. Geol.*, 142(3–4), 141–173.

Gilbert, G. K. (1909), The convexity of hilltops, *J. Geol.*, 17, 344–350.

Green, E. G., W. E. Dietrich, and J. F. Banfield (2003), The quantification of mass loss via geochemical weathering in hillslope processes, *Eos Trans. AGU*, 84(46), Fall Meet. Suppl., Abstract H51E-1128.

Heimsath, A. M., W. E. Dietrich, K. Nishiizumi, and R. C. Finkel (1997), The soil production function and landscape equilibrium, *Nature*, 388(6640), 358–361.

Heimsath, A. M., W. E. Dietrich, K. Nishiizumi, and R. C. Finkel (1999), Cosmogenic nuclides, topography, and the spatial variation of soil depth, *Geomorphology*, 27(1–2), 151–172.

Hirano, M. (1976), Mathematical model and the concept of equilibrium in connection with slope shear ration, *Z. Geomorphol.*, 25, 50–71.

Howard, A. D. (1994), A detachment-limited model of drainage-basin evolution, *Water Resour. Res.*, 30(7), 2261–2285.

Howard, A. D. (1997), Badland morphology and evolution: Interpretation using a simulation model, *Earth Surf. Processes Landforms*, 22(3), 211–227.

Jyotsna, R., and P. K. Haff (1997), Microtopography as an indicator of modern hillslope diffusivity in arid terrain, *Geology*, 25(8), 695–698.

Keller, E. A., R. L. Zepeda, T. K. Rockwell, T. L. Ku, and W. S. Dinklage (1998), Active tectonics at Wheeler Ridge, southern San Joaquin Valley, California, *Geol. Soc. Am. Bull.*, 110(3), 298–310.

Kirkby, M. J. (1967), Measurement and theory of soil creep, *J. Geol.*, 75(4), 359–378.

Kirkby, M. J. (1971), Hillslope process-response models based on the continuity equation, *Inst. Br. Geogr. Spec. Publ.*, 3, 15–30.

Kirkby, M. J. (1977), Soil development models as a component of slope models, *Earth Surf. Processes Landforms*, 2(2–3), 203–230.

Kirkby, M. J. (1985), A basis for soil-profile modeling in a geomorphic context, *J. Soil Sci.*, *36*(1), 97–121.

Kooi, H., and C. Beaumont (1994), Escarpment evolution on high-elevation rifted margins: Insights derived from a surface processes model that combines diffusion, advection, and reaction, *J. Geophys. Res.*, *99*(B6), 12,191–12,209.

Koons, P. O. (1989), The topographic evolution of collisional mountain belts—A numerical look at the Southern Alps, New Zealand, *Am. J. Sci.*, *289*(9), 1041–1069.

Mckean, J. A., W. E. Dietrich, R. C. Finkel, J. R. Southon, and M. W. Caffee (1993), Quantification of soil production and downslope creep rates from cosmogenic Be-10 accumulations on a hillslope profile, *Geology*, *21*(4), 343–346.

Millot, R., J. Gaillardet, B. Dupre, and C. J. Allegre (2002), The global control of silicate weathering rates and the coupling with physical erosion: New insights from rivers of the Canadian Shield, *Earth Planet. Sci. Lett.*, *196*(1–2), 83–98.

Nepstad, D. C., C. R. Decarvalho, E. A. Davidson, P. H. Jipp, P. A. Lefebvre, G. H. Negreiros, E. D. Dasilva, T. A. Stone, S. E. Trumbore, and S. Vieira (1994), The role of deep roots in the hydrological and carbon cycles of Amazonian forests and pastures, *Nature*, *372*(6507), 666–669.

Pazzaglia, F. J., and T. W. Gardner (1994), Late Cenozoic flexural deformation of the middle U. S. Atlantic passive margin, *J. Geophys. Res.*, *99*(B6), 12,143–12,157.

Rinaldo, A., W. E. Dietrich, R. Rigon, G. K. Vogel, and I. Rodriguez-Iturbe (1995), Geomorphological signatures of varying climate, *Nature*, *374*, 632–635.

Roering, J. J., J. W. Kirchner, and W. E. Dietrich (1999), Evidence for nonlinear, diffusive sediment transport on hillslopes and implications for landscape morphology, *Water Resour. Res.*, *35*(3), 853–870.

Roering, J. J., J. W. Kirchner, and W. E. Dietrich (2001), Hillslope evolution by nonlinear, slope-dependent transport: Steady state morphology and equilibrium adjustment timescales, *J. Geophys. Res.*, *106*(B8), 16,499–16,513. (Correction, *J. Geophys. Res., 106*(B11), 26,787–26,789.)

Sander, H. (2002), The porosity of tropical soils and implications for geomorphological and pedogenetic processes and the movement of solutions within the weathering cover, *Catena*, *49*(1–2), 129–137.

Small, E. E., R. S. Anderson, and G. S. Hancock (1999), Estimates of the rate of regolith production using Be-10 and Al-26 from an alpine hillslope, *Geomorphology*, *27*(1–2), 131–150.

Stonestrom, D. A., A. F. White, and K. C. Akstin (1998), Determining rates of chemical weathering in soils—Solute transport versus profile evolution, *J. Hydrol.*, *209*(1–4), 331–345.

Summerfield, M. A., and N. J. Hulton (1994), Natural controls of fluvial denudation rates in major world drainage basins, *J. Geophys. Res.*, *99*(B7), 13,871–13,883.

Tucker, G. E., and R. L. Bras (1998), Hillslope processes, drainage density, and landscape morphology, *Water Resour. Res.*, *34*(10), 2751–2764.

Tucker, G. E., and R. Slingerland (1996), Predicting sediment flux from fold and thrust belts, *Basin Res.*, *8*(3), 329–349.

White, A. F., A. E. Blum, M. S. Schulz, D. V. Vivit, D. A. Stonestrom, M. Larsen, S. F. Murphy, and D. Eberl (1998), Chemical weathering in a tropical watershed, Luquillo Mountains, Puerto Rico: I. Long-term versus short-term weathering fluxes, *Geochim. Cosmochim. Acta*, *62*(2), 209–226.

White, A. F., A. E. Blum, T. D. Bullen, D. V. Vivit, M. Schulz, and J. Fitzpatrick (1999), The effect of temperature on experimental and natural chemical weathering rates of granitoid rocks, *Geochim. Cosmochim. Acta*, *63*(19–20), 3277–3291.

Willett, S. D., R. Slingerland, and N. Hovius (2001), Uplift, shortening, and steady-state topography in active mountain belts, *Am. J. Sci.*, *301*(4–5), 455–485.

Willgoose, G., R. L. Bras, and I. Rodriguez-Iturbe (1991), A coupled channel network growth and hillslope evolution model: 1. Theory, *Water Resour. Res.*, *27*(7), 1671–1684.

————————————

D. J. Furbish, Department of Civil and Environmental Engineering, Vanderbilt University, VU Station B 351831, 2301 Vanderbilt Place, Nashville, TN 37235-1831, USA. (david.j.furbish@vanderbilt.edu)

S. M. Mudd, Department of Earth and Environmental Sciences, Vanderbilt University, VU Station B 357805, 2301 Vanderbilt Place, Nashville, TN 37235-1805, USA. (simon.m.mudd@vanderbilt.edu)